environmental microbiology

Environmental Microbiology (2021) **23**(8), 4576–4594 doi:10.1111/1462-2920.15651

Dynamics of Baltic Sea phages driven by environmental changes

Matthias Hoetzinger,[1*] Emelie Nilsson,[1] Rahaf Arabi,[1] Christofer M. G. Osbeck,[1] Benjamin Pontiller,[1] Geoffrey Hutinet,[2] Oliver W. Bayfield,[3] Sachia Traving,[4] Veljo Kisand,[5] Daniel Lundin,[1] Jarone Pinhassi,[1] Mathias Middelboe[6] and Karin Holmfeldt[1]**

[1]*Centre for Ecology and Evolution in Microbial Model Systems (EEMiS), Department of Biology and Environmental Science, Linnaeus University, Kalmar, Sweden.*

[2]*Department of Microbiology and Cell Science, University of Florida, Gainesville, FL.*

[3]*York Structural Biology Laboratory, Department of Chemistry, University of York, York, UK.*

[4]*Nordcee and HADAL, Department of Biology, University of Southern Denmark, Odense, Denmark.*

[5]*Institute of Technology, University of Tartu, Tartu, Estonia.*

[6]*Marine Biological Section, Department of Biology, University of Copenhagen, Helsingør, Denmark.*

Summary

Phage predation constitutes a major mortality factor for bacteria in aquatic ecosystems, and thus, directly impacts nutrient cycling and microbial community dynamics. Yet, the population dynamics of specific phages across time scales from days to months remain largely unexplored, which limits our understanding of their influence on microbial succession. To investigate temporal changes in diversity and abundance of phages infecting particular host strains, we isolated 121 phage strains that infected three bacterial hosts during a Baltic Sea mesocosm experiment. Genome analysis revealed a novel Flavobacterium phage genus harboring gene sets putatively coding for synthesis of modified nucleotides and glycosylation of bacterial cell surface components. Another novel phage genus revealed a microdiversity of phage species that was largely maintained during the experiment and across mesocosms amended with different nutrients. In contrast to the newly described Flavobacterium phages, phages isolated from a *Rheinheimera* strain were highly similar to previously isolated genotypes, pointing to genomic consistency in this population. In the mesocosm experiment, the investigated phages were mainly detected after a phytoplankton bloom peak. This concurred with recurrent detection of the phages in the Baltic Proper during summer months, suggesting an influence on the succession of heterotrophic bacteria associated with phytoplankton blooms.

Received 18 December, 2020; accepted 11 June, 2021. For correspondence. *E-mail matthias.hotzinger@lnu.se; Tel. +46 704761047. **E-mail karin.holmfeldt@lnu.se; Tel. +46 480447310.

Introduction

Bacteriophages are estimated to lyse 10%–20% of marine heterotrophic bacteria each day (Suttle, 1994). The specificity of phage infection entails fundamental implications on microbial community composition and succession. Besides the direct effects on bacterial mortality rates, there are also indirect effects, most notably, the release of organic matter that is subsequently available for recycling by prokaryotes rather than being channeled to higher trophic levels (Wilhelm and Suttle, 1999). Although the pivotal role of phages in this context is unquestioned, relatively few studies have focused on resolving the ecology of specific phage-host relations in natural marine environments (Kang *et al*., 2013; Zhao *et al*., 2013; Marston and Martiny, 2016; Alonso-Sáez *et al*., 2018). The resulting interdependencies and dynamics of specific phages and their hosts within microbial communities are thus largely unknown. There is a limited amount of data on the densities and population dynamics of aquatic phages that are obtained by isolation, and thus can be reliably linked to a host (Holmfeldt *et al*., 2007; Kang *et al*., 2013; Zhao *et al*., 2013; Marston and Martiny, 2016), compared to the vast amount of community sequencing data available (Hurwitz and Sullivan, 2013; Brum *et al*., 2015; Coutinho *et al*., 2017; Gregory *et al*., 2019). Thus, specific information on temporal dynamics gained from phage isolates may benefit the analysis of community sequencing data and the understanding of microbial succession patterns.

Extensive data on the seasonal dynamics of bacteria and eukaryotic phytoplankton are available from the Baltic Sea.

Time series data at the Linnaeus Microbial Observatory (LMO) located in the Baltic Proper showed that microbial succession patterns recurred over multiple years (Bunse *et al*., 2019). Time-series samples from 2011 to 2014 revealed pronounced phytoplankton blooms in spring, characterized by high biomass of dinoflagellates and diatoms. The spring bloom supported an increase in bacterial abundance that usually peaked in August, after a serrated development with multiple fluctuations. Cyanobacterial blooms were recurring during the summer months, under stratified conditions between June and September (Bunse *et al*., 2019). In contrast to the well-characterized dynamics of cellular microbes in the Baltic Sea, relatively little is known about how phages respond to and influence microbial succession patterns. Phage isolates available from the Baltic Sea show little genome sequence similarity to sequenced viruses from other environments (Holmfeldt *et al*., 2013; Šulčius and Holmfeldt, 2016; Nilsson *et al*., 2019, 2020). Even phages isolated from the same bacterial strain may exhibit remarkable genomic diversity. There are examples of multiple taxa sharing little or no detectable sequence similarity that can infect the same host strain (Holmfeldt *et al*., 2013). Four novel genera of Flavobacterium (Bacteroidetes) phages isolated from LMO surface water were characterized recently, including two different genera isolated from the same host strain. Only one of the novel genera was detected at LMO in a metagenome time series from 2012 to 2015 (Nilsson *et al*., 2020). Another phage genus that was isolated and detected in the viral metagenomes from the same site is the *Barbavirus* that infects a *Rheinheimera* strain (*Gammaproteobacteria*). This phage showed a clear seasonal pattern with increased relative abundance in August and September each year in the LMO time series, similar to its host according to an amplicon dataset (Nilsson *et al*., 2019). Yet, studies linking phage–host dynamics to environmental conditions are necessary in order to incorporate phages into a more holistic picture on microbial succession in the Baltic Sea.

In this study, we isolated phages from 121 plaques obtained during a mesocosm experiment prepared with water from LMO. Genome sequencing revealed two novel Flavobacterium phage genera as well as phages with high similarity to the above-mentioned Rheinheimera phages. We characterized their genomes, their diversity during the mesocosm experiment, and temporal abundance variations over three consecutive years at LMO.

Experimental procedures

Isolation of bacteria

Eleven bacterial strains isolated from the Baltic Proper were used as potential hosts for phage isolation through plaque assays. Two of the strains for which phages were obtained, *Rheinheimera* sp. BAL341 and *Flavobacterium* sp. LMO8, were described previously (Nilsson *et al*., 2019, 2020). The third strain that yielded phage plaques, *Flavobacterium* sp. BAL314, was isolated following the procedure used for isolating *Rheinheimera* sp. BAL341 (Nilsson *et al*., 2019). Water for isolation of strain BAL314 was collected on 24 May 2012, at 2 m depth at the LMO, situated 10 km off the coast of eastern Öland in the Baltic Sea (56°55′51.24″ N, 17°3′38.53″ E). The strains that did not yield any plaques were *Algoriphagus* sp. BAL317, *Algoriphagus* sp. BAL319, *Brevundimonas* sp. BAL450, *Cellulophaga* sp. OL12a (Holmfeldt *et al*., 2007), *Flavobacterium* sp. LMO6 (Nilsson *et al*., 2020), *Polaribacter* sp. BAL337, *Psychrobacter* sp. BAL309 and *Sphingomonas* sp. BAL323. Strains BAL317, BAL319, BAL309, BAL323 were isolated in May 2012, strain BAL337 in July 2012, and strain BAL450 in February 2013 from surface water collected at LMO and isolated as described in Nilsson *et al*. (2019).

Isolation of phages

Water for viral isolation was collected from a mesocosm experiment (30 May–8 June 2016) that was described in detail elsewhere (paper III in Osbeck, 2019). Briefly, each mesocosm contained 160 L of 100 μm filtered water collected on 30 May at 2 m depth from LMO (11.7°C, salinity 7.2 g/kg), mixed with 40 L of 0.2 μm filtered treatment-specific water. Five different treatments were established in triplicate and manipulated with respect to inorganic nutrient concentrations and sources of organic matter, resulting in a total of 15 mesocosms. The treatment-specific water was obtained from the humic river Lapväärti (62°14′21″ N, 21°34′38″ E) that discharges into the Baltic Sea in Finland (Humi), the agricultural-influenced river Lielupe (56°48′42″ N 23°35′5″ E) that discharges into the Baltic Sea in Latvia (Agri), LMO water amended with nitrogen ($NaNO_3$), phosphorus (Na_2HPO_4), and silicate ($NaSiO_3$) corresponding to final concentrations of 16, 1, and 32 μM respectively (NPSi), LMO water amended with 10 ml of sonicated and centrifuged 0.22 μm filtered cyanobacterial lysate of *Nodularia spumigena* strain AV1 containing 21 300 μg L^{-1} chlorophyll-*a* (Cyan), and a control from LMO without nutrient amendments (Cont). Each mesocosm was covered by a transparent Plexiglas plate to reduce the risk of contamination, stirred regularly to prevent stratification, and bubbled with air to maintain oxygen saturation. The water temperature in all mesocosms was between 14 and 15°C during the whole experiment. A 12 h light–dark cycle was provided at a flux density of ~400 μmol photons m^{-2} s^{-1}. Bacterial abundance and chlorophyll-*a* concentration were determined daily during the experiment, and additionally 6 h after the experiment started, as described previously (paper III in Osbeck, 2019).

Samples for isolation of phages were collected daily during the mesocosm experiment. For phage isolation, 10 ml of water was filtered through a 0.2 μm syringe filter (Merck Millipore, Darmstadt, Germany). The filtered water was then used directly for phage isolation by plaque assays with the 11 bacterial strains mentioned above. Host bacteria were grown overnight in liquid Zobell medium {1 g yeast extract [Becton, Dickinson and Company (BD), Franklin Lakes, NJ, USA] and 5 g Bacto peptone (BD) in 800 ml of 1.2 μm filtered (GF/C Whatman glass microfiber filter, GE Healthcare, Chicago, IL, USA) Baltic Sea water and 200 ml of Milli-Q water} with gentle agitation. The bacterial culture (300 μl) was mixed with 400 μl of the 0.2 μm filtered mesocosm water and 3.5 ml molten top agar {marine sodium magnesium buffer (MSM): 450 mM NaCl, 50 mM $MgSO_4 \cdot 7H_2O$, 50 mM Tris [Trizma base (Sigma, St. Louis, MO, USA)], pH 8; with 0.5% low melting point agarose (Thermo Fisher Scientific, Waltham, MA, USA)}. The mixture was spread evenly onto Zobell agar plates [15 g L^{-1} bacto agar (BD)], incubated at room temperature, and inspected for visible plaques after 1–4 days. In the case of plaque formation, the number of plaque-forming units (PFU) was counted after plaques were clearly visible. Phages were isolated by picking individual plaques with a sterile 100 μl pipette tip, which was thereafter submerged in MSM to disperse the phages and centrifuged at 20 000*g* for 5–10 min to remove bacterial cells. The supernatant containing the phages was then re-plated as described above, but this time by mixing 300 μl of bacterial culture with 100 μl of phage culture. The procedure was repeated three times. Pure isolates were harvested by adding 5 ml MSM to fully lysed plates, the top-agar layer was shredded with an inoculation loop, and the plate incubated on a shaking table (40 rpm) for at least 30 min. The phages suspended in MSM were collected into a falcon tube, centrifuged for 10 min at 2860*g*, filtered through a 0.2 μm syringe filter, and stored at 4°C for further characterization.

Host range tests

Phage isolates elemoA_7-9A, elemoD_13-5B and immuto_2-6A were tested on eight *Flavobacteriaceae* strains (BAL38, BAL304, BAL314, BAL330, BAL346, LMO6, LMO8 and LMO9), which previously have been isolated from LMO surface water. Bacteria were grown overnight, mixed with top agar and spread on agar plates as described above. Ten microliters of phage stock was pipetted into the molten top agar and streaked across the molten top agar with sterile pipette tips according to the Molten Streaking for Singles method (Kauffman and Polz, 2018) modified as described in Nilsson *et al*. (2020). Plates were incubated at room temperature and inspected for plaque formation in the bacterial lawn after 4 days. Tests were conducted two times for each phage–bacterium pair.

DNA extraction and genome sequencing of phages and hosts

Phage DNA was extracted using the Wizard PCR DNA Purification kit (Promega, Madison, WI, USA) and DNA of *Flavobacterium* sp. BAL314 was isolated using the EZNA tissue DNA kit (Omega Bio-tek, Norcross, GA, USA), following the procedures described in Nilsson *et al*. (2019) for phage and bacterial DNA isolation respectively. The DNA was sequenced at SciLife/NGI (Solna, Sweden). The Nextera XT Kit (Illumina, San Diego, CA, USA) was used for library preparation. Paired-end (2 × 125 bp) sequencing was performed on a HiSeq 2500 instrument (Illumina).

Morphological characterization of phages

Transmission electron microscopy was conducted on high-titre phage lysate. Carbon–formvar-coated copper grids (Agar Scientific, Essex, UK) were plasma cleaned in a PELCO easiGlow for 60 s at 0.38 mbar (air) and 20 mA. Lysate (5 μl) was applied to a grid for 60 s and thereafter removed by wicking. The grid was washed with deionized water (5 μl) and stained with 5 μl of 2% wt./vol. uranyl acetate (Agar Scientific). Grids were imaged using an FEI Tecnai 12 G2 BioTWIN microscope with tungsten filament operating at 120 kV. Phage particles were measured using ImageJ v2.0.0.

Genome assembly, annotation, and analysis

Raw reads of the *Flavobacterium* sp. BAL314 genome were quality trimmed and adapter sequences removed using Trimmomatic v0.30 (Bolger *et al*., 2014) (settings: -PE -phred33 ILLUMINACLIP:nextera_linkers.txt:2:30:10 LEADING:3 TRAILING:3 SLIDINGWINDOW:4:15 MINLEN:30), and quality was evaluated using FastQC (Andrews, 2010). Trimmed reads were assembled using Spades v3.6.0 (Bankevich *et al*., 2012) with k-mer lengths of 21, 33, 55, 77 and 99. The genome was annotated using the IMG Annotation pipeline v5.5.0 (Markowitz *et al*., 2012), and screened for prophage sequences using the Phaster webserver (Arndt *et al*., 2016). Genome assembly and annotation of *Rheinheimera* sp. BAL341 and *Flavobacterium* sp. LMO8 was described in Nilsson *et al*. (2019) and Nilsson *et al*. (2020)) respectively.

Phage genomes were assembled using the same method as for the bacteria, resulting in one contig with overlapping ends of 99 bp (used k-mer length for assembly) for each genome. The overlapping sequences were

removed at one end to circularize the genomes. Inter-genomic similarities among phages were calculated using the VIRIDIC webserver (Moraru *et al*., 2020). Average nucleotide identities (ANI) for both bacterial and phage genomes were calculated using the ANIb method in Pyani v0.2.7 (Pritchard *et al*., 2015).

Open reading frames (ORFs) in the phage genomes were called using Phanotate v1.2.2 with default settings (McNair *et al*., 2019). The pan-genome of the phages from each of the three bacterial strains was inferred using Roary v3.12.0 (Page *et al*., 2015) with a 70% amino acid sequence identity threshold. The largest genome of each of the three groups was used as reference for annotation, and ORFs present in the pan-genome but absent in the reference were added. For annotation of the phage ORFs, amino acid sequences were aligned against current (October 2019) releases of the databases referred to in the following: Search against the NCBI non-redundant (nr) database (Agarwala *et al*., 2018) using Diamond v0.9.26 (Buchfink *et al*., 2015) in sensitive mode, alignment against the virus-specific databases NCBI RefSeq viral protein (Agarwala *et al*., 2018) and Phantome phage proteins (http://www.phantome.org) using blastp v2.5.0+ (Camacho *et al*., 2009), and HMM search against the pVOGs database (Grazziotin *et al*., 2017) using jackhmmer (http://hmmer.org/). Specific genes (e.g. those involved in queuosine biosynthesis) were further compared to the protein data bank (Berman *et al*., 2000) using the HHpred server (Zimmermann *et al*., 2018) with default settings. An *e*-value cutoff of 0.0001 was used for all alignments. The best three hits of each alignment approach were manually inspected to decide on the gene annotations; hits annotated as hypothetical protein or unknown function were omitted. Assignments to COG (Tatusov *et al*., 2000) and Pfam (Finn *et al*., 2010) IDs were adopted from results obtained through the IMG Annotation pipeline v5.5.0 (Markowitz *et al*., 2012). The tRNAscan-SE v2.0 webserver (Lowe and Chan, 2016) was used for identification of tRNAs.

Phage genomes were screened for integrases, excisionases and partitioning genes parA (found in extrachromosomal temperate phages) as signs of a potential lysogenic lifestyle. Ribonucleotide reductase (RNR) genes present in the genome of phage immuto_2-6A and its bacterial host strain LMO8 were analyzed by HMM search against the RNRdb database (Lundin *et al*., 2009) using HMMER v3.1b2.

Phylogenetics

To identify the *Flavobacterium* hosts, their 16S rRNA gene sequences were blasted against GenBank (Agarwala *et al*., 2018) and sequences of isolated strains with more than 95% sequence identity were collected. Furthermore, respective sequences of the strains used in the host range tests were added and the 16S rRNA gene sequence of *Polaribacter marinaquae* strain RZW3-2 was used as an outgroup. Sequences were aligned with MAFFT v7 (Katoh and Standley, 2013) using the 'ginsi' option. The alignment was trimmed to a length of 1349 bp, and the phylogenetic tree was calculated using RAxML v8 with the rapid hill-climbing algorithm, the GTRGAMMA nucleotide substitution model and 1000 bootstrap replicates (Stamatakis, 2014).

For phylogenetic analysis of the phages, publicly available phage genomes to which alignments of protein sequences with *e*-values <0.0001 were obtained during annotation (see above) were selected as references. Furthermore, the IMG/ER database was screened for reference phage genomes that shared sequence similarity to the reference phages elemoA_7-9A and immuto_2-6A. Pairwise comparisons of the nucleotide genome sequences were conducted using the Genome-BLAST Distance Phylogeny (GBDP) method with the formula D0 implemented on the VICTOR webserver (Meier-Kolthoff and Göker, 2017). The resulting inter-genomic distances were used to infer a balanced minimum evolution tree with branch support via FASTME including SPR postprocessing (Lefort *et al*., 2015). Branch support was inferred from 100 pseudo-bootstrap replicates.

Inferring abundances of phages and their hosts in environmental samples

Reads from viral metagenomes (<0.2 μm size fraction, viruses aggregated using iron chloride and collected on 1 μm filters) sampled at LMO between 2012 and 2015 [BioProject accession number: PRJNA474405 (Nilsson *et al*., 2019)] were mapped separately against the genomes of elemoA_7-9A, immuto_2-6A and barba_13-8A using bowtie2 (Langmead and Salzberg, 2012) with the settings '--ignore-quals --mp 1,1 --np 1 --rdg 0,1 --rfg 0,1 --score-min L,0,-0.05' to apply a sequence identity threshold of 95%. Selected metagenomes were mapped a second time against the three phage genomes after changing the '--score-min' parameters to 'L,0,-0.2' to apply a sequence identity threshold of 80% in order to determine if specific regions of the genomes not covered in the first run would be covered at lower identity. The 'map-bowtie2-markduplicates.sh' script, which is part of the MetAssemble software package (https://github.com/inodb/metassemble), was used to calculate coverage depth and the percentage of the genomes covered by metagenome reads. Average coverage depth across the genomes was divided by metagenome size in gigabases (Gb) to obtain average depth per Gb of metagenome (referred to as depth per Gb later on).

Reads from bacterial metagenomes (0.2–3.0 μm size fraction) sampled at LMO between 2012 and 2015 [BioProject accession numbers: PRJNA273799 (Hugerth *et al*., 2015) and PRJEB34883 (Alneberg *et al*., 2020)] were mapped against the genomes of the bacterial host strains BAL314 and LMO8 in the same way as described for the phages above. Linear regression parameters between relative abundances (depth per Gb) of phages and their hosts in LMO metagenomes were calculated using the lm function from the stats v3.6.3 package in R (R Core Team, 2019). Spearman's rank correlations were calculated using the cor.test function from the same package. Correlations were determined for different time lags (see Fig. S2), e.g. phage abundance in a certain sample was associated with host abundance in a sample taken several days earlier. As LMO metagenomes were not sampled at constant time intervals, the time points that were associated for one correlation do not all have the exact same time difference but were allowed to vary within the range of 1 week. Amplicon datasets from LMO samples taken between 2012 and 2015 (BioProject accession number: PRJEB42455), containing sequences of the 16S rRNA gene V3–V4 region from two filter size fractions (0.2–3.0 and >3.0 μm), were used to track an amplicon sequencing variant (ASV) identical to the respective sequence of both strains BAL314 and LMO8. The amplicon sequencing procedure was described in Nilsson *et al*. (2019). Read processing and downstream analysis was performed by following the ampliseq pipeline v1.2.0dev (Straub *et al*., 2020) (settings: 'trunclenf 259, trunclenr 199, --double_primer') using cutadapt v2.6. (Martin, 2011) and qiime v2019.10.0 (Bolyen *et al*., 2019).

Accession numbers

The assembled genomes of the elemo-, immuto- and barba-phages were deposited to NCBI under the accession numbers MT497017 and MT497065–MT497125, MW353175–MW353177 and MT497224–MT497279 respectively. The *Flavobacterium* sp. BAL314 genome is available in the IMG/ER database (Markowitz *et al*., 2012) under the genome ID 2821289949. The genomes of *Flavobacterium* sp. LMO8 (accession: NZ_WIBJ00000000) and Rheinheimera sp. BAL341 (accession: CAAJGR010000000) were previously deposited to NCBI and EMBL/ENA respectively.

Results and discussion

Characteristics of the bacterial hosts

Rheinheimera sp. BAL341 and *Flavobacterium* sp. LMO8 were described earlier (Karlsson *et al*., 2019; Nilsson *et al*., 2020). Like strain LMO8, *Flavobacterium* sp. BAL314 formed round, yellow to orange colonies on agar plates. Its genome assembled into 35 contigs >1 kilobase (kb), accounting for 2.82 megabases (Mb). According to publicly available 16S rRNA gene sequences, the phylogenetically closest relatives to BAL314 were LMO8 and two other isolates from the Baltic Sea, BAL38 and LMO6 (Fig. 1). Despite high 16S rRNA gene sequence similarities among these isolates (99.5%–99.8% identity), genome-wide dissimilarities were substantial. The ANI between BAL314 and BAL38, LMO6, and LMO8 was 94%, 94% and 85% over an alignment fraction (AF) of 77%, 75% and 62% respectively. This suggests that at least LMO8 is associated with a different species than BAL314, while BAL38 and LMO6 are close to the borderline for grouping them into the same species as BAL314 according to the suggested threshold of 95%–96% ANI for species delineation (Richter and Rosselló-Móra, 2009). *Flavobacterium* sp. LMO8 shared an ANI of 85% over an AF of 62% with both BAL38 and LMO6. Similar to LMO8 (Nilsson *et al*., 2020), the Phaster software detected no prophage region within the genome of BAL314.

Phage isolation

Plaques were obtained on three out of the eleven tested bacterial strains, the *Flavobacterium* strains BAL314 and LMO8, and the *Rheinheimera* strain BAL341 (Fig. 2A–C; Table S1). For isolation of phage strains, 216, 76 and 67 plaques on BAL314, LMO8 and BAL341, were initially picked respectively. For the phages of LMO8 and BAL341, attempts were made to purify all initially picked plaques, however, only 3 and 56 phages respectively, passed three rounds of re-plating. Due to the large number of originally isolated phages for BAL314 and time constraints, we purified phage plaques from days 1, 3, 5 and 9 of the mesocosm experiment. Of those, 62 phages passed three rounds of re-plating. All 121 purified phage strains were genome sequenced.

Genomic relatedness and phylogeny of the isolated phages

Minimum intergenomic similarity among the 62 phages that infected *Flavobacterium* strain BAL314 was 85.3% (Table S2). Comparisons to publicly available genomes revealed low relatedness. Highest similarity was found to be to Cellulophaga phage phi19:1, a Flavobacteriaceae siphovirus isolated from the Baltic Sea (Holmfeldt *et al*., 2007, 2013), with 2.2% intergenomic similarity. This suggests that the phages isolated on strain BAL314 represent a novel genus. Based on a 95% genome similarity

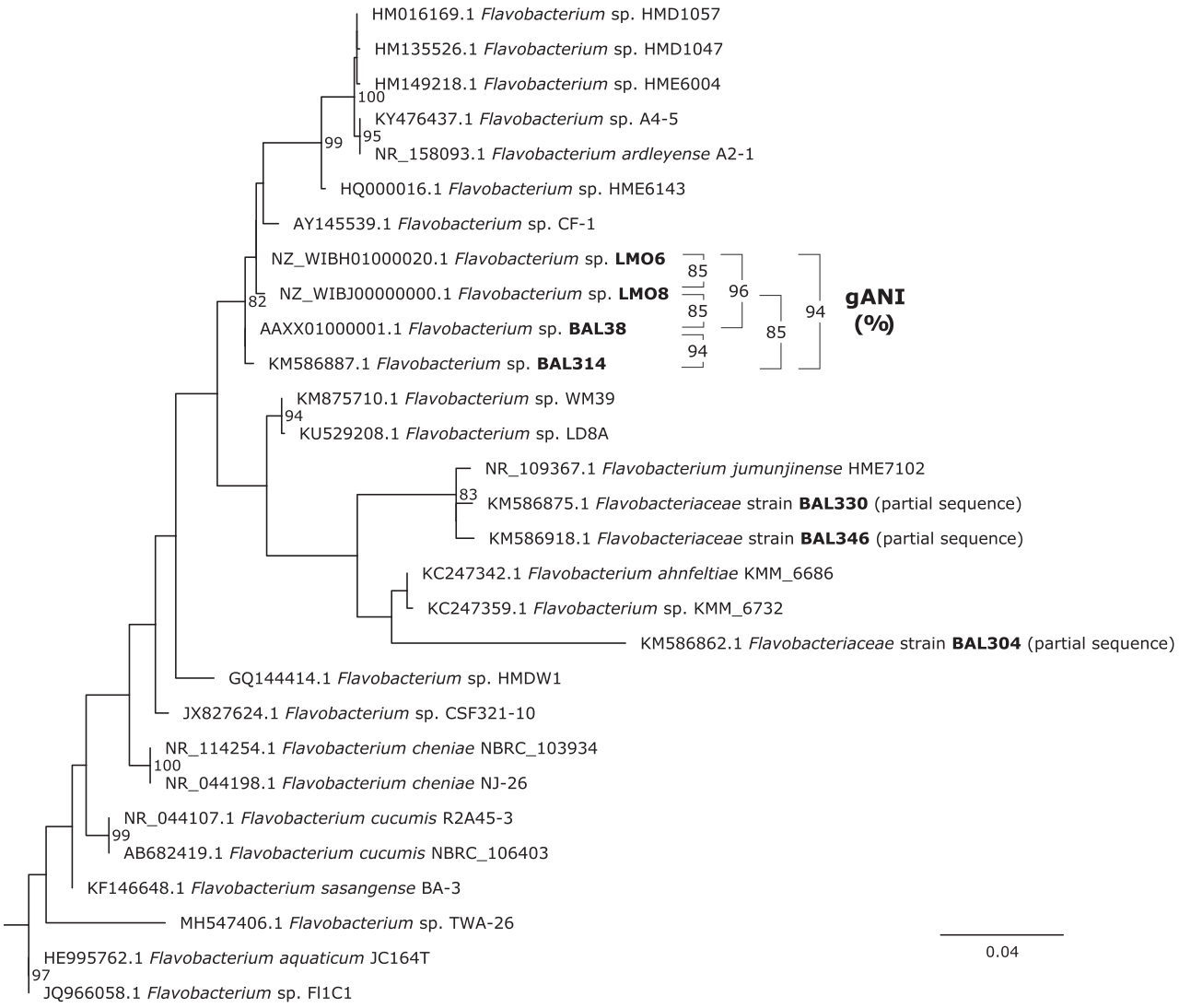

Fig. 1. Phylogeny of *Flavobacterium* strains based on 16S rRNA gene sequences. The tree is rooted using the sequence of *Polaribacter marinaquae* strain RZW3-2 as an outgroup, which is not shown. Bootstrap values >80% are shown. Strains that were isolated from the Baltic Proper and were used for host range tests are in bold font. Note that strain LMO9 is not shown as its 16S rRNA gene sequence is identical to that of strain LMO6. Genome-wide average nucleotide identities (ANI) among the host strains (BAL314 and LMO8) of phages isolated in this study and their most closely related strains are given.

threshold, VIRIDIC clustered the 62 strains into six different species (Table S2). We indicated these species in the GBDP tree (Fig. 3). We propose the name Elemovirus for the genus, referring to the LMO sampling station being the source of isolation of both the phage and its host. The six species will be named Flavobacterium virus ElemoA, Flavobacterium virus ElemoB, and so on, and the strains, e.g. vB_FspP_elemoA_7-9A, according to the ICTV's recommendations (Kropinski *et al*., 2009). The prefix 'vB' indicates that it is a bacterial virus, 'Fsp' designates the host species (*Flavobacterium* sp.), 'P' the viral family based on morphology (*Podoviridae*), and 'elemoA_7-9A' provides the specific strain designation. The strain designation is composed of the species name, the mesocosm number (1–3: Cont, 4–6: NPSi, 7–9: Humi, 10–12: Agri, 13–15: Cyan) from which the phage was isolated (before the hyphen), and the day of the experiment when it was isolated (after the hyphen). The letter at the end of the designation was added to distinguish between different phages isolated from the same mesocosm and on the same day but from different plaques. Within this article, phage strains are not referred to by their full name but by their specific strain designation only.

The genomes of the three phages isolated on the *Flavobacterium* strain LMO8 showed a minimum intergenomic similarity of 99.2% (Table S2) and were not

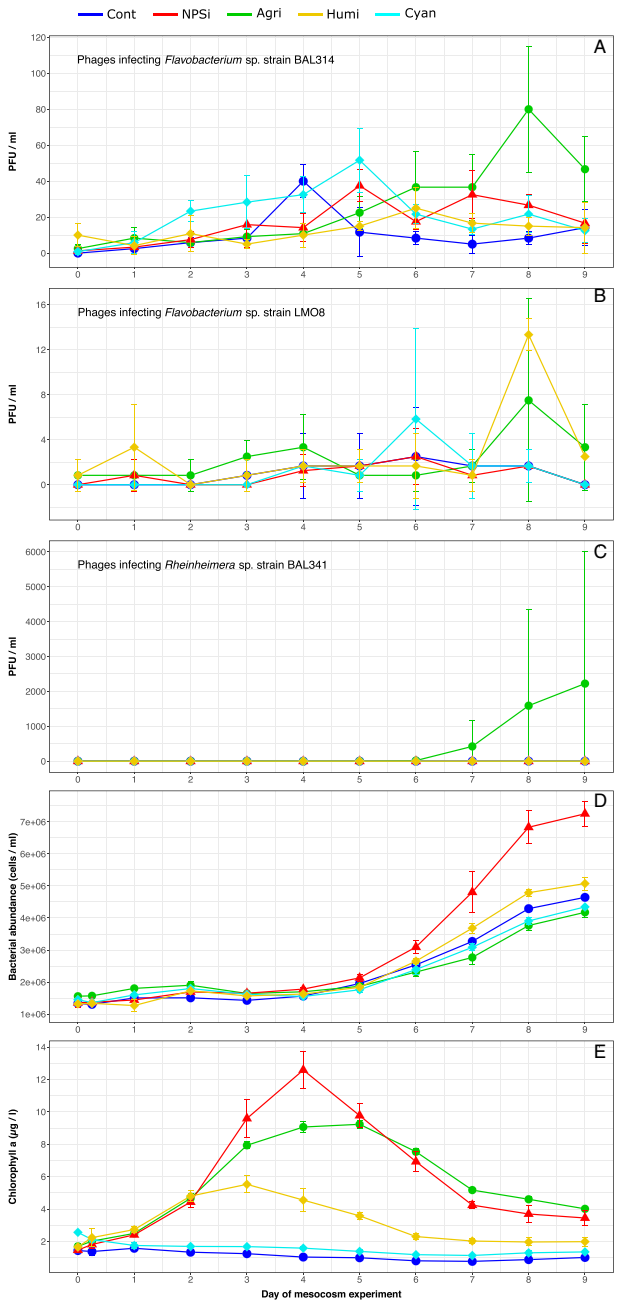

Fig. 2. Dynamics during the mesocosm experiment. Temporal development of infective phage abundances (PFU counts; note the different scales on the *y*-axes) on three bacterial strains (A–C), total bacterial abundance (D) and chlorophyll-*a* concentration (E) in the five mesocosm treatments containing 100 µm filtered LMO water and 20% of the following treatment-specific water (Cont: 0.22 µm filtered LMO water; NPSi: 0.22 µm filtered LMO water and additional nitrogen, phosphorus and silicate; Agri: 0.22 µm filtered agriculture-influenced Lielupe river water; Humi: 0.22 µm filtered humic Lapäarti river water; Cyan: 0.22 µm filtered LMO water) amended with a cyanobacterial lysate of *Nodularia spumigena*. Average values from triplicated mesocosms are shown. Error bars depict standard deviations. PFU values for the individual mesocosms are shown in Supplemental Table S1. [Color figure can be viewed at wileyonlinelibrary.com]

related (<0.1% intergenomic similarity) to phages previously isolated from the same host strain (genera *Tant-* and *Pippivirus*, Nilsson *et al*., 2020). The most similar published phage genome was an uncultured single-amplified genome, vSAG 37-F16 retrieved from the Mediterranean Sea (Martinez-Hernandez *et al*., 2017), exhibiting a genome similarity of 5.1% to the three phages isolated on LMO8. Hence, no closely related phage genomes have been described so far, and accordingly, VIRIDIC assigned these phages to the same species within a novel genus (Table S2). As the genomes harbored a high proportion of genes putatively involved in cell surface modification and a gene set for biosynthesis of modified nucleosides, we propose the name Immutovirus (from *immutare*, Latin verb for 'change, alter, transform') for the genus. Consequently, the species name is Flavobacterium virus Immuto, and the full strain name is, e.g. vB_FspM_immuto_2-6A.

Minimum intergenomic similarity among the 56 Rheinheimera phage isolates was 96.8% (Table S3). Based on intergenomic similarities, 31 of the phages were assigned to the previously described species Rheinheimera virus Barba18A and the remaining 25 to Rheinheimera virus Barba21A (Table S3; Fig. S1) of the genus *Barbavirus* (Nilsson *et al*., 2019). The previously described barba-phages were isolated using the same host strain, and some of them shared a genome similarity of 100.0% with phages isolated in this study (Table S3).

Phage-host specificity

Phages previously isolated on *Flavobacterium* LMO8 were able to infect two other *Flavobacterium* strains, although these only shared 85% ANI with the original host (Nilsson *et al*., 2020). In contrast, immuto_2-6A isolated on LMO8 in this study did not infect any of the tested *Flavobacteriaceae* strains apart from its original host. Similarly, elemoA_7-9A and elemoD_13-5B did not infect any strain but its original host, *Flavobacterium* BAL314, despite this strain sharing 94% ANI with three of the tested bacterial strains (Fig. 1). While these results certainly do not exclude the possibility that the immuto- and elemo-phages infect other bacteria than their hosts of isolation, it suggests that these phages do not commonly cross-infect different *Flavobacterium* species and might exhibit higher host specificity compared to phages isolated on LMO8 previously.

Genomic features of the isolated phages

A general description of the phages is presented in the Supplementary Material (Text S1). In addition to typical

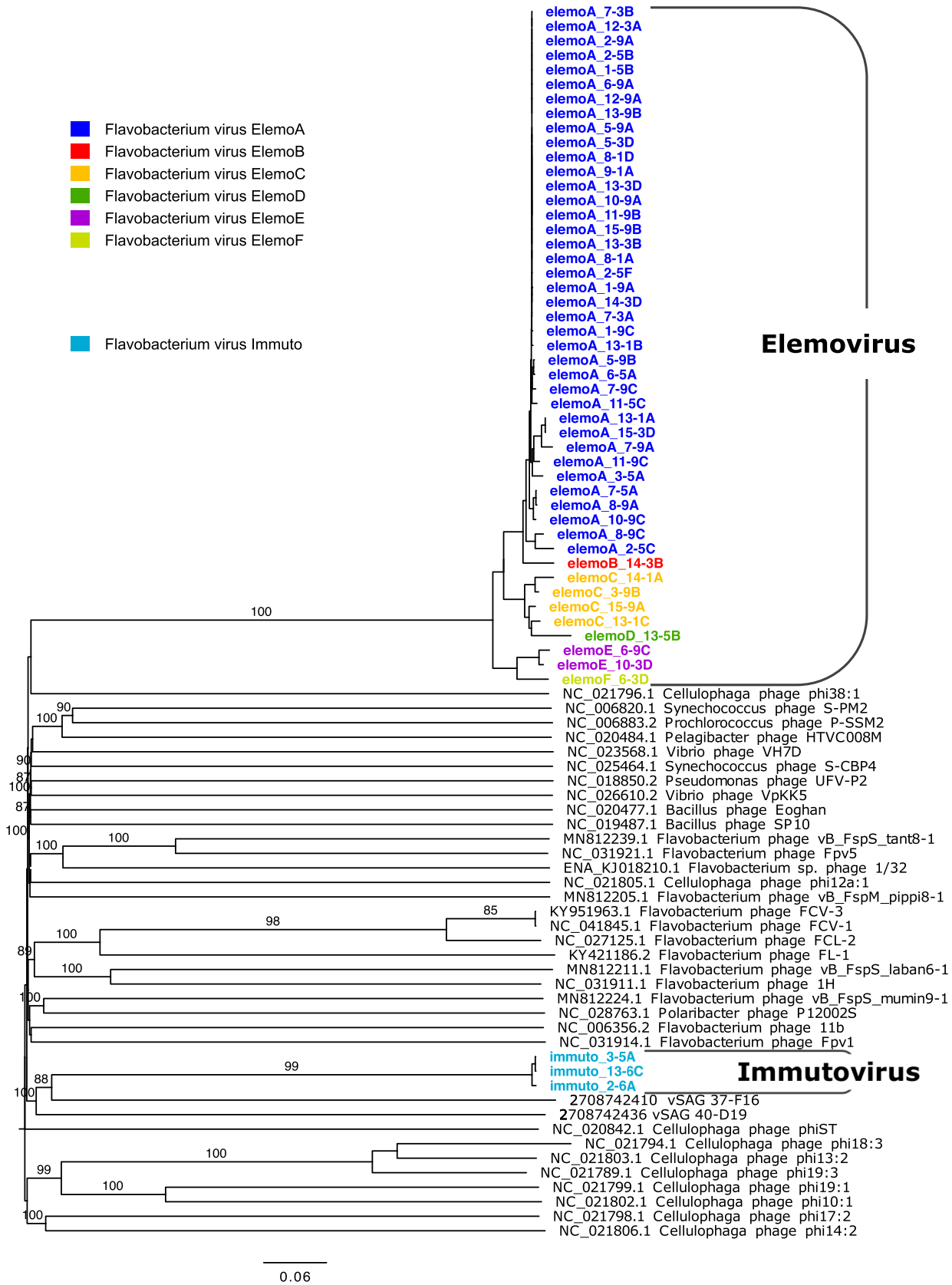

Fig. 3. Legend on next page.

phage DNA replication and morphogenesis genes, the 160 kb large immuto-phage genomes (Fig. 4; Table S4) contained a set of nucleotide metabolism genes (folE, queC, queD, queE and queF) that are part of the queuosine (Q) biosynthesis pathway in bacteria and archaeosine (G^+) biosynthesis in archaea. Queuosine is incorporated into certain tRNAs of bacteria and eukaryotes, where it is assumed to modulate translation and was also shown to protect tRNAs against cleavage by ribonucleases (Wang *et al*., 2018). Archaeosine modifies archaeal tRNA and is considered to stabilize its three-dimensional structure (Turner *et al*., 2020). Only recently it has been demonstrated that the G^+ base and precursors of the Q base modify phage genomic DNA and thereby protect it from host restriction systems (Hutinet *et al*., 2019). The gene set found in immuto_2-6A was suggested to catalyze the synthesis of either the Q base precursor 7-aminomethyl-7-deazaguanine ($preQ_1$) or the G^+ base. Phages harboring a similar gene set are Streptococcus phage Dp-1, Cellulophaga phage phi3ST:2 and Vibrio phage phi-ST2 (Hutinet *et al*., 2019). Further analyses are needed to determine if immuto_2-6A produces similar guanosine modifications and if the phage is protected from host restriction. Another striking feature of the immuto-phage genomes was a 10.8 kb long gene cassette containing various genes putatively involved in glycosylation of bacterial cell surface components, amongst others, four glycosyltransferases, a nucleotide-diphosphate-sugar epimerase and two dTDP-4-amino-4,-6-dideoxygalactose transaminases (Fig. 4; Table S4). Similar gene sets are typically found in hypervariable genomic islands of bacteria, where they affect phage recognition by modifying extracellularly exposed glycopolymers (Rodriguez-Valera *et al*., 2009; Avrani *et al*., 2011; Li *et al*., 2015; Rodriguez-Valera *et al*., 2016). Variability in such genomic islands within populations of free-living prokaryotes entails strain-specific phage predation, which could be crucial for maintaining microdiversity (Rodriguez-Valera *et al*., 2009), and is assumed to be realized through frequent horizontal replacement of the island (López-Pérez *et al*., 2014; Rodriguez-Valera *et al*., 2016). The presence of a resemblant genomic island in the immuto-phages might indicate that they are involved in its distribution through gene transfer, or in structuring the bacterial cell surface directly through the expression of these genes. The latter is known from human-pathogenic bacteria and their lysogenic phages that encode glycosyltransferases that can alter the serotype of the bacterium in a process termed serotype conversion (Iseki and Sakai, 1953; Allison and Verma, 2000), thereby evading the immune system of the human host. More generally, natural selection is assumed to preserve outer membrane biogenesis genes encoded by phages, as cell surface modification may prevent detrimental super-infection by related phages during the lysogenic life cycle (Markine-Goriaynoff *et al*., 2004). However, no genes potentially involved in genome integration or excision were identified in the immuto-phage genomes, and also the clear plaques produced by the immuto-phages during replication do not point towards lysogeny. The assumed fitness advantage of phage-encoded cell surface modification genes through prevention of super-infection may be questioned for a lytic phage exhibiting a relatively short intracellular life cycle. It has been proposed that modification of the host's outer membrane by phage-encoded glycosyltransferases may benefit the phage after lytic infection as it inhibits virion retention on cell debris (Markine-Goriaynoff *et al*., 2004). If such a selective advantage explains the presence of the respective gene set in the immuto-phage genomes or if its presence has a different reason remains an open question.

The immuto-phages furthermore contained genes encoding a RNR, which catalyzes the reduction of ribonucleotides to the corresponding deoxyribonucleotides. Interestingly, predicted RNR genes belonged to the NrdAi/NrdBi phylogenetic subclass, while the RNR genes present in the host genome (*Flavobacterium* sp. LMO8) were characterized as NrdAe/NrdBe subclass (Nouairia et al., in preparation). Both subclasses are common among *Flavobacteriaceae* bacteria but clearly separated phylogenetically (Harrison *et al*., 2019; Martínez-Carranza *et al*., 2020). Thus, the phage might have acquired its RNR genes from another *Flavobacterium* host that differed from strain LMO8 regarding its RNR genes. NrdAi genes are lacking an ATP cone domain, which is present in many other RNR subclasses including NrdAe (Harrison *et al*., 2019; Martínez-Carranza *et al*., 2020), and acts as a regulatory switch that inactivates the enzyme upon dATP binding (Hofer *et al*., 2012). It has been suggested that RNRs without an ATP cone are beneficial for fast-replicating lytic phages as they cannot be inactivated through dATP binding (Harrison *et al*., 2019).

In contrast to the diverse functional genes harbored by the immuto-phages, no metabolic genes were detected among the elemo-phages (Fig. 5; Tables S5 and S6). Even RNR genes, which are prevalent particularly among

Fig. 3. Genome-BLAST distance phylogeny of phages isolated on *Flavobacterium* strains BAL314 and LMO8. Bootstrap values >80% are shown. The phages isolated from BAL314 represent the novel genus Elemovirus, those isolated from LMO8 the genus Immutovirus. The elemo-phages were subdivided into six species indicated by different colours. [Color figure can be viewed at wileyonlinelibrary.com]

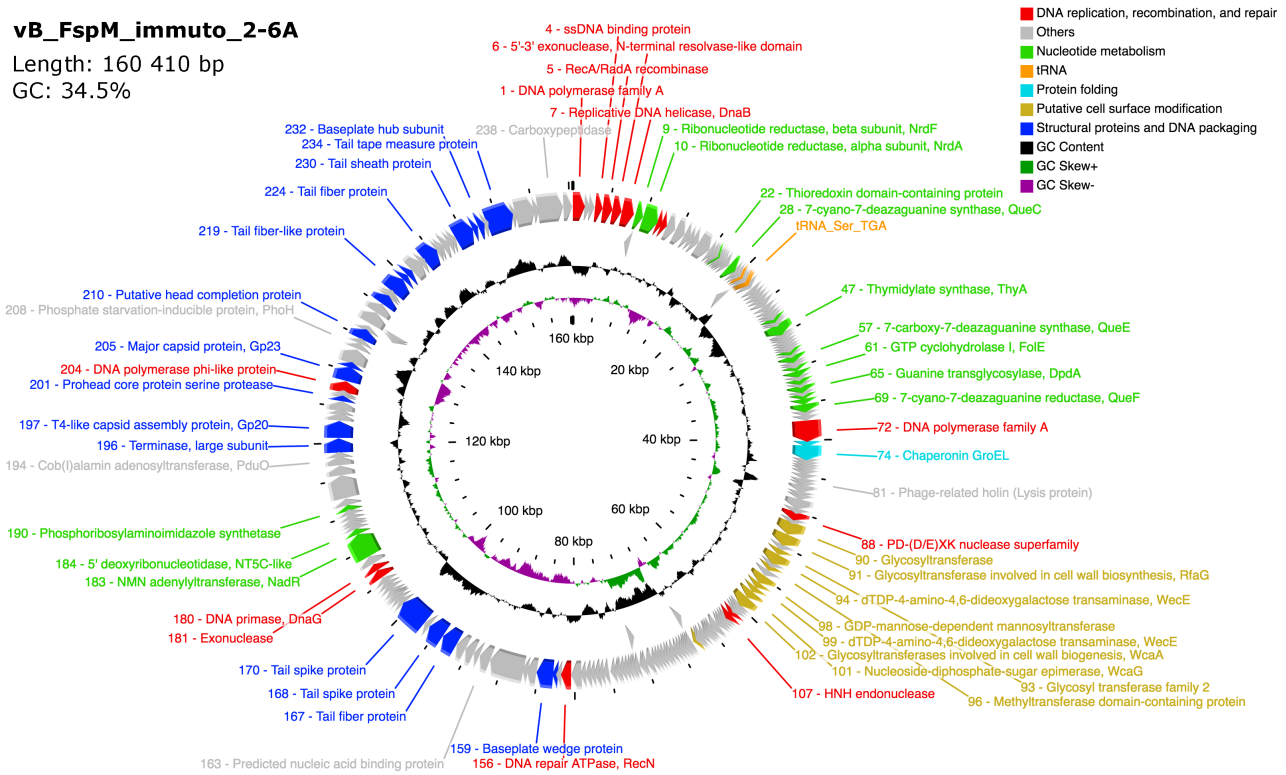

Fig. 4. Genome annotation of vB_FspM_immuto_2-6A. Genes encoded on one strand are represented by clockwise arrows, genes encoded on the opposite strand by counterclockwise arrows. Genes that could be assigned to specific functional categories are shown in the respective colour. The complete annotation is given in Table S4. [Color figure can be viewed at wileyonlinelibrary.com]

aquatic phages (Holmfeldt *et al*., 2013), were absent. Yet, the lack of metabolic genes does not seem to prevent ecological success of the elemo-phages that showed higher relative abundances in the Baltic Proper compared to the other phages in this study (see below). Annotation of the barba-phages did not reveal novel functions for this taxon, that is, all genes in the pan-genome of the phages isolated in this study either had their best hit to genes annotated in the previously isolated barba-phages or could only be annotated as 'hypothetical proteins' (Table S7).

Phage morphology

The short tails of the elemo-phages (Fig. 6A and B; Text S1) classify them as podoviruses. The barba-phages isolated in this study all showed intergenomic similarity ≥97.3% with barba18A (Table S3) that was previously classified as a myovirus (Fig. 3 in Nilsson *et al*., 2019). Due to the high genomic similarity, it is assumed that the morphologies of the phages from this study are similar and thus no additional characterization was performed. The immuto-phages are also classified as myoviruses (Fig. 6C and D; Text S1). A gene consisting of 1006 amino acids present in the immuto-phage annotated as tape measure protein (TMP) allowed for investigation of the proposed association between TMP and tail length (Katsura and Hendrix, 1984) in this phage. We further expanded the empirical basis for the correlation between TMP and tail length (Katsura and Hendrix, 1984; Abuladze *et al*., 1994; Pedulla *et al*., 2003; Mahony *et al*., 2016) to various myo- and siphoviruses by analyzing publicly available data (Fig. 6E; Table S8). The TMP assumedly forms an α-helical protein that functions as template during tail assembly (Katsura and Hendrix, 1984). The observed slope of the regression line of 0.144 nm/AA (Fig. 6E) is close to a theoretical slope of 0.147 nm/AA, which is the average length of an amino acid in an extended α-helix (Mahony *et al*., 2016). Thus, the TMP allows for a reasonable prediction of tail length for different sipho- as well as myoviruses, including the immuto-phage.

Dynamics of the phages in the mesocosms

The phages that infected the three different host strains all showed a general trend to increase in abundance (PFU count) towards the end of the experiment, coinciding with an increase in overall bacterial abundance and a decrease in chlorophyll-*a* concentration after a peak in

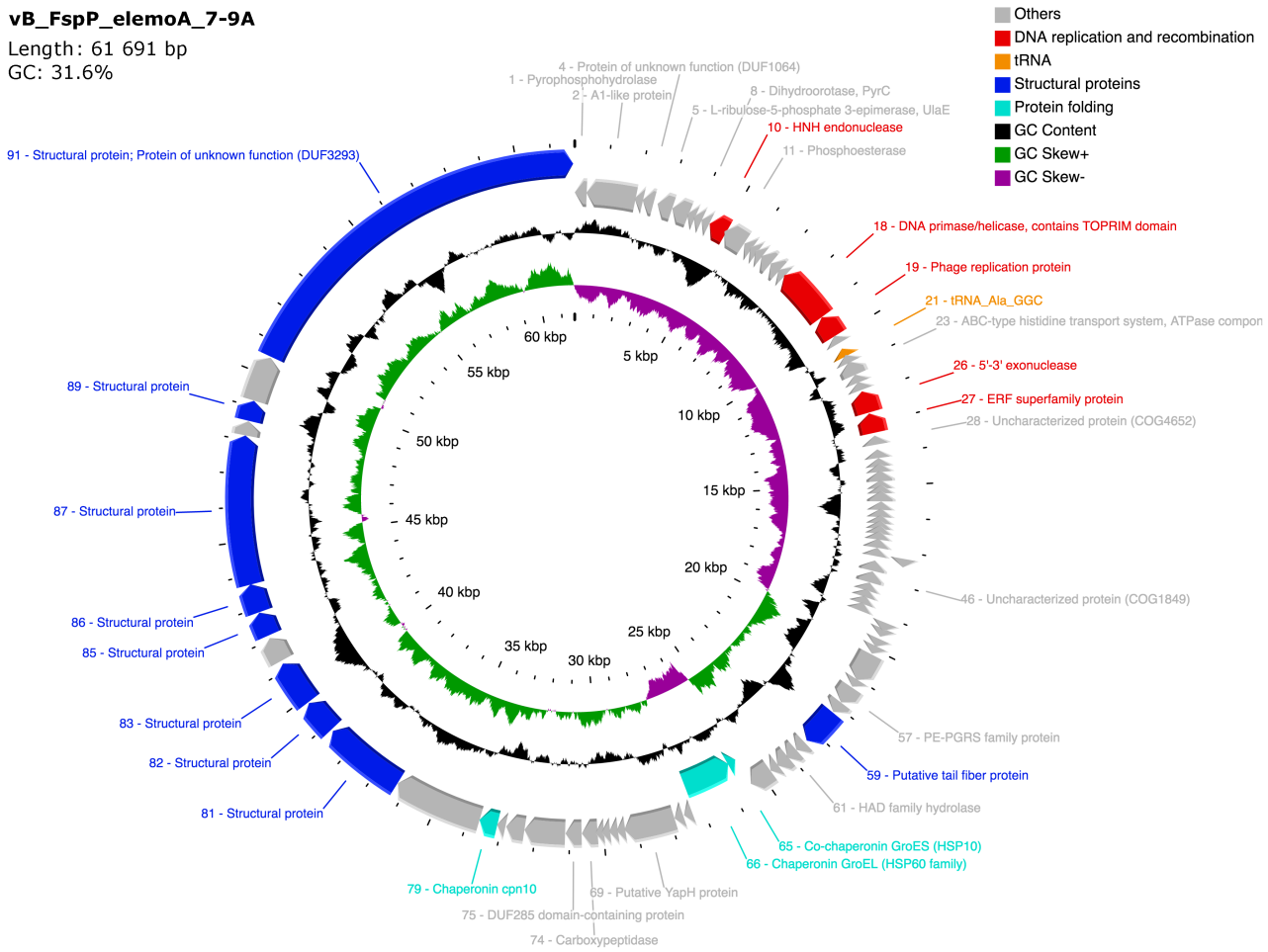

Fig. 5. Genome annotation of vB_FspP_elemoA_7-9A. The genome is illustrated similarly as in Fig. 4. Genes are more evenly distributed across both strands and the GC skew is more pronounced compared to the immuto_2-6A genome. The complete annotation is given in Table S5. [Color figure can be viewed at wileyonlinelibrary.com]

the NPSi, Agri and Humi mesocosms (Fig. 2). Yet, the plaque counts revealed pronounced differences regarding their abundance in the different mesocosms, suggesting that their specific hosts responded differently to the treatments, thus driving the temporal variations in phage abundance.

The phages of BAL314 showed dynamics in all mesocosms reaching their maximum abundance in the Agri mesocosms (Fig. 2A), indicating a positive response of the host to substrate input from the agricultural influenced river. The maximum density of 105 plaques ml^{-1} was detected on day 8 of the experiment after the chlorophyll-*a* peak had declined (Fig. 2E). The second highest PFU increase was in the Cyan treatment, where PFU counts were high earlier in the experiment compared to the other treatments and reached its maximum of 68 plaques ml^{-1} on day 5. This suggests a positive response of BAL314 to cyanobacterial lysis products that may have also supported the growth in the Agri treatment after phytoplankton bloom demise. This agrees with previous observations for certain *Flavobacteriaceae* bacteria, i.e. growth response to phytoplankton blooms (Pinhassi *et al*., 2004) and high proportions of *Flavobacterium* strains obtained from growth media enriched with cyanobacterial hepatotoxins (Berg *et al*., 2009).

The phages that infected LMO8 showed an overall low abundance throughout the mesocosms (Fig. 2B), which corresponds to the low relative abundance of immuto-phages in the natural environment compared to the abundance seen for the elemo-phages that infect BAL314 (see below). The LMO8 phages were most abundant in the Humi mesocosms (up to 17.5 plaques ml^{-1}), which may suggest a preference of the host for humic-rich water.

Phages of *Rheinheimera* BAL341 were rarely detected in most samples (Fig. 2C) yet showed a surprisingly strong response in one Agri mesocosm replicate (increasing from 55 plaques ml^{-1} on day 6 to 6600 plaques mL^{-1} on day

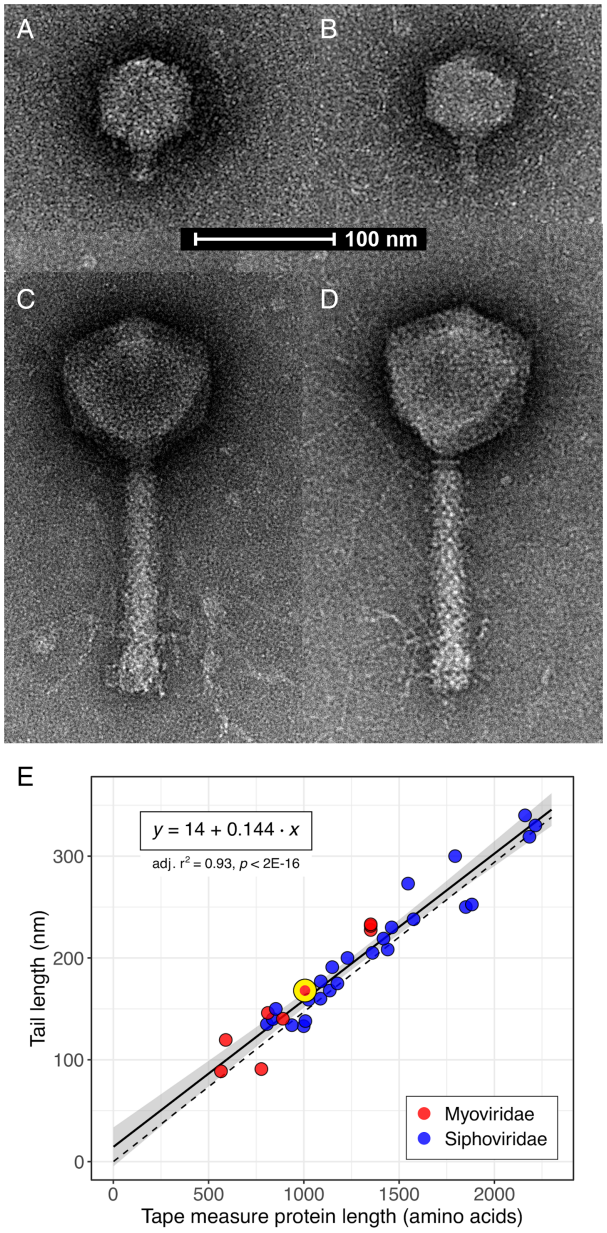

Fig. 6. Phage morphology. Transmission electron microscopy (TEM) micrographs of elemoA_7-9A (A) and elemoD_13-5B (B) showing a podovirus morphology. Measurements of multiple virions revealed similar sizes for both strains (capsid diameter ~75 nm, tail length ~18 nm, Supplemental Text S1). Micrographs of immuto_2-6A (C, D) revealing a myovirus morphology (capsid diameter ~115 nm, tail length ~168 nm, sheath length ~133 nm, tail width ~25 nm, Supplemental Text S1). The scale bar is the same for all four micrographs. The correlation between TMP length and tail length of various phages with sipho- and myovirus morphology is shown in (E). The dashed line shows a theoretical relation between tail and TMP length of 0.147 nm/AA as expected from an extended α-helical protein (see main text). Note that this line is drawn through the origin for simplicity, although phages are expected to deviate upwards, as tail length may exceed tail tube length (Katsura and Hendrix, 1984) or downwards, as not all residues of the TMP may be part of the actual tape protein (Mahony *et al*., 2016). The empirically obtained regression is given as a solid line with the 95% confidence interval in grey. Immuto_2-6A is highlighted in yellow. [Color figure can be viewed at wileyonlinelibrary.com]

9), followed by a delayed response in a second Agri replicate (increase from 10 plaques ml^{-1} on day 8 to 70 plaques ml^{-1} on day 9). It is not clear what stimulated this increase in the BAL341 phages, but *Rheinheimera* bacteria have previously been observed to profit from environmental changes in Baltic Sea microcosm experiments (Lindh *et al*., 2015). The barba-phages infecting BAL341 that were previously described were isolated in August and September 2015 from LMO surface water and have shown recurrent patterns in abundance during these late summer months from 2012 to 2015 (Nilsson *et al*., 2019). Thus, it appears that the barba-phages in the Baltic Sea are sustained at low levels during most times of the year and that rapid responses in abundance are induced by host blooms naturally occurring after phytoplankton blooms during late summer (Nilsson *et al*., 2019). The phytoplankton bloom in the Agri-treatment in our mesocosm experiment simulated these naturally occurring events. The lack of detected barba-phages in LMO metagenomes during late spring (see Fig. 8C), when water for the mesocosm experiment was collected, could explain the few barba-phage plaques during the first 5 days of the experiment.

The emergence of initially undetected phage populations in response to the treatments agrees with the few previous studies that have investigated shifts in overall viral diversity during mesocosm experiments (Øvreås *et al*., 2003; Sandaa *et al*., 2009). Within these studies, Pulsed Field Gel Electrophoresis (PFGE) has been used to monitor the shifts in viral diversity in response to changing environmental conditions. As PFGE only provides information on genome sizes of viruses in a community, the information regarding shifts of particular viral populations is limited as different viruses might have the same genome size. Consequently, further investigations on the dynamics of specific phage populations are needed to gain a better understanding of viral community responses to nutrient amendments.

Host-specific diversity of the isolated phages in the mesocosms

The elemo-phages revealed a noticeable microdiversity and differentiated into six species (Fig. 3) according to the VIRIDIC results (Table S2), with a minimum intergenomic similarity of 85.3% between elemoD_13-5B and elemoE_6-9C. The intergenomic differences are mainly attributable to gene content differences, while sequence dissimilarity among homologous regions is minor within the 62 elemo-phages, indicated by a high minimum ANI of 97.5% (note that ANI refers to nucleotide identity among homologous genes, while intergenomic similarity as calculated by VIRIDIC takes both shared genome content and sequence similarity into account). The pangenome of the 62 elemo-phages contained 110 genes of

which 78 were core genes (present in all phages, Table S5) and 32 accessory genes (not present in all phages, Table S6). Among the eight accessory genes that could be annotated with putative functions, two were annotated as replication proteins and six as HNH endonucleases or other genes putatively involved in recombination. While this suggests a high propensity of recombination among elemo-phages that shapes the accessory genome, gene annotation did not provide hints on potential ecological differences among the different species. Nevertheless, one species (ElemoA) appeared to be overrepresented throughout the mesocosm experiment but did not seem to be promoted or impeded by any of the different treatments (Fig. 7A). The other species were represented by four or fewer isolates in total, distributed over different time points and treatments without a clear pattern (Fig. 7A). Thus, a treatment-specific response of particular species could not be observed. Considering the overall species diversity within the different treatments, the Cyan treatment revealed the highest diversity with four different species represented by 18 genome-sequenced isolates, while the Humi treatment showed the lowest diversity, with all 14 genome-sequenced isolates assigned to the same species (ElemoA). Further investigations are necessary to test if these differences in diversity between the treatments are consistent, and if so, clarify the underlying mechanisms.

The phages isolated from *Rheinheimera* BAL341 were predominantly obtained from the Agri treatment, which probably illustrates a treatment-specific response of the host. During the strong increase in abundance, particularly in the Agri mesocosm after day 6 (Fig. 2C), two species within the same genus showed similar proportions among the sequenced genomes (Fig. 7B). Thus, like for the elemo-phages, no marked changes in species diversity were observed for the barba-phages throughout the experiment. Interestingly, isolates of these two species had already been obtained from LMO 9 months before the water for the mesocosm experiment was collected (Fig. S1). This suggests that individual viral species can be maintained over long periods and across changing environmental conditions and that the barba-phages form a genomically consistent population in the Baltic Sea, which has previously been suggested through the mapping of metagenomes (Nilsson *et al*., 2019).

For phages infecting LMO8, it is unclear if their overall diversity differed depending on treatment, given that we could isolate only three phages with almost identical genomes. Unlike the BAL341 phages, which were highly similar to phages previously isolated on that host, the LMO8 phages were dissimilar (<0.1% intergenomic similarity) to *Tant*- and *Pippivirus*, two different genera that had previously been isolated on the LMO8 host (Table S2). While these previously isolated phage genera potentially could have been among the identified plaques that did not pass through purification, this is unlikely due to the differences in plaque morphology. All originally counted plaques from the mesocosm samples displayed the same, tiny plaque morphology (dots, <1 mm), which differed from the plaque morphology of the previously known LMO8 phages (1–3 mm). Notably, phages for LMO8 have been isolated in low abundances compared to phages for other hosts during the same investigations (this study and Nilsson *et al*., 2020), suggesting a low abundance in the Baltic Proper, where they may exist at the detection limit for conventional plaque assay methods. Detection of the immuto-phages in viral metagenomes from LMO, where the maximum relative abundance was more than an order of magnitude lower than that of the elemo-phages (see below, Fig. 8), supports this assumption.

Overall, the observed diversity of phages from each of the three host strains was rather limited during this experiment. Despite the noticeable microdiversity within the elemo-phages, only one phage genus was obtained for each host strain. This contrasts observations of other phage-host systems, e.g. Cellulophaga phages from the Baltic Sea, including examples of multiple phage genera isolated using the same host strain and the same water sample (Holmfeldt *et al*., 2007, 2013), but is similar to what has previously been seen for phages infecting *Rheinheimera* (Nilsson *et al*., 2019) and *Flavobacterium* strains LMO6 and LMO9 (Nilsson *et al*., 2020), which were all isolated from LMO. Within each phage population, consisting of viruses infecting the same host, the microdiversity did not shift throughout the experiment. Instead, the proportions of different species remained reasonably constant despite changes in abundance. This contrasts previous investigations of viral population-level diversity in response to environmental stressors in mesocosms, where the population diversity of *Emiliania huxleyi* viruses decreased throughout the experiments (Schroeder *et al*., 2003; Highfield *et al*., 2017). However, different environmental factors affecting the dynamics of the phototrophic *E. huxleyi* host populations and heterotrophic bacterial host populations respectively, might contribute to explaining the different development in viral diversity. Further investigations are needed to clarify how environmental changes affect the diversity of phages infecting particular host strains and how such effects influence the diversity of whole populations.

Dynamics of the isolated phage taxa in the Baltic Sea

The relative abundance of the phages isolated from the mesocosm experiment was followed at LMO in the Baltic Sea in a time series from April 2012 to December 2014 by mapping viral metagenomes (<0.2 μm fraction) against

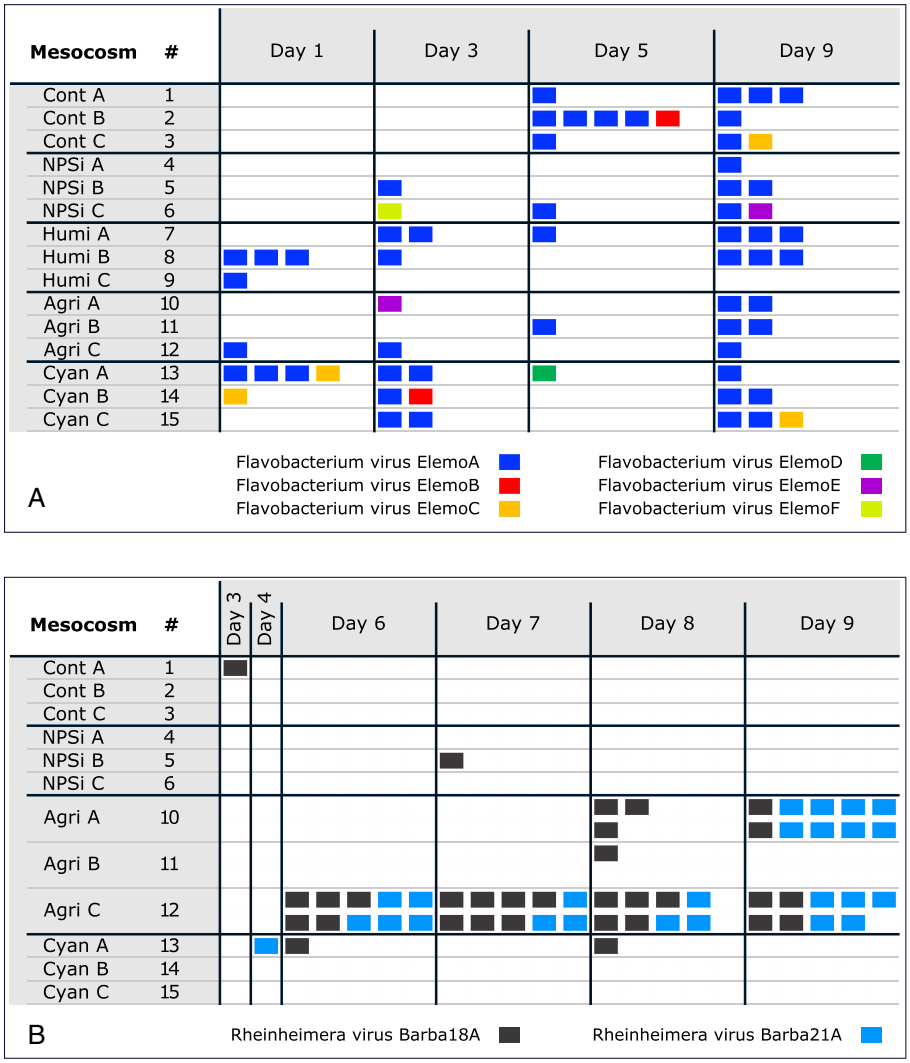

Fig. 7. Diversity of phages isolated during the mesocosm experiment. All genome-sequenced elemo-phages isolated from *Flavobacterium* strain BAL314 (A) and barba-phages isolated from *Rheinheimera* strain BAL341 (B) are shown. Each filled rectangle represents a genome, coloured according to the assigned host species. Rows and columns indicate the mesocosm from which it was obtained and the timepoint of the sampling respectively. [Color figure can be viewed at wileyonlinelibrary.com]

the genomes of elemoA_7-9A, immuto_2-6A and barba_13-8A (Fig. 8A–C). The relative abundances are given as 'genome-wide average depth of mapped bases per Gb of metagenome' (e.g. compare Fig. 5 in Bischoff *et al*., 2019), referred to as depth per Gb for simplicity. This is equivalent to the also commonly used 'bp mapped per kb of genome per Mb of metagenome' (e.g. compare Fig. 4 in Brum *et al*., 2015). Elemo-phages were markedly more abundant than immuto- and barba-phages, with a maximum depth per Gb of 25.8 in July 2013 compared to maximum 2.1 and 1.1 depth per Gb of the latter respectively. The percentage of the genome covered by mapped reads verifies their detection. Roux et al. (2017) suggested to consider a viral genome detected in a sample if more than 75% of it is covered by metagenomic reads. Accordingly, both elemo- and immuto-phages were detected in all seasons except for winter, from which fewer samples were available. In comparison, the previously described phage genera *Tant-* and *Pippivirus* isolated from LMO8 were not detected in this time series, although they were isolated from the same site (Nilsson *et al*., 2020). While the immuto-phages showed a more erratic detection pattern, the elemo-phages showed a seasonal pattern and were detected each year during summer (Fig. 8; Table S9). To put the observed relative abundances of elemo-phages into context, the numbers can be compared to those from previously published studies mapping marine viral metagenomes against phage genomes (Brum *et al*., 2015; Bischoff *et al*., 2019). For instance, the majority of genomes assembled from Tara Ocean viral metagenomes were found with relative abundances between 1 and 10 depth per Gb when metagenomes were mapped back to the assembled contigs (Brum *et al*., 2015). Assuming that the genomes retrieved from metagenome assembly represent the abundant phage populations of a sample, this suggests that elemo-phages detected at depth per Gb of up to 25.8 (Fig. 8A)

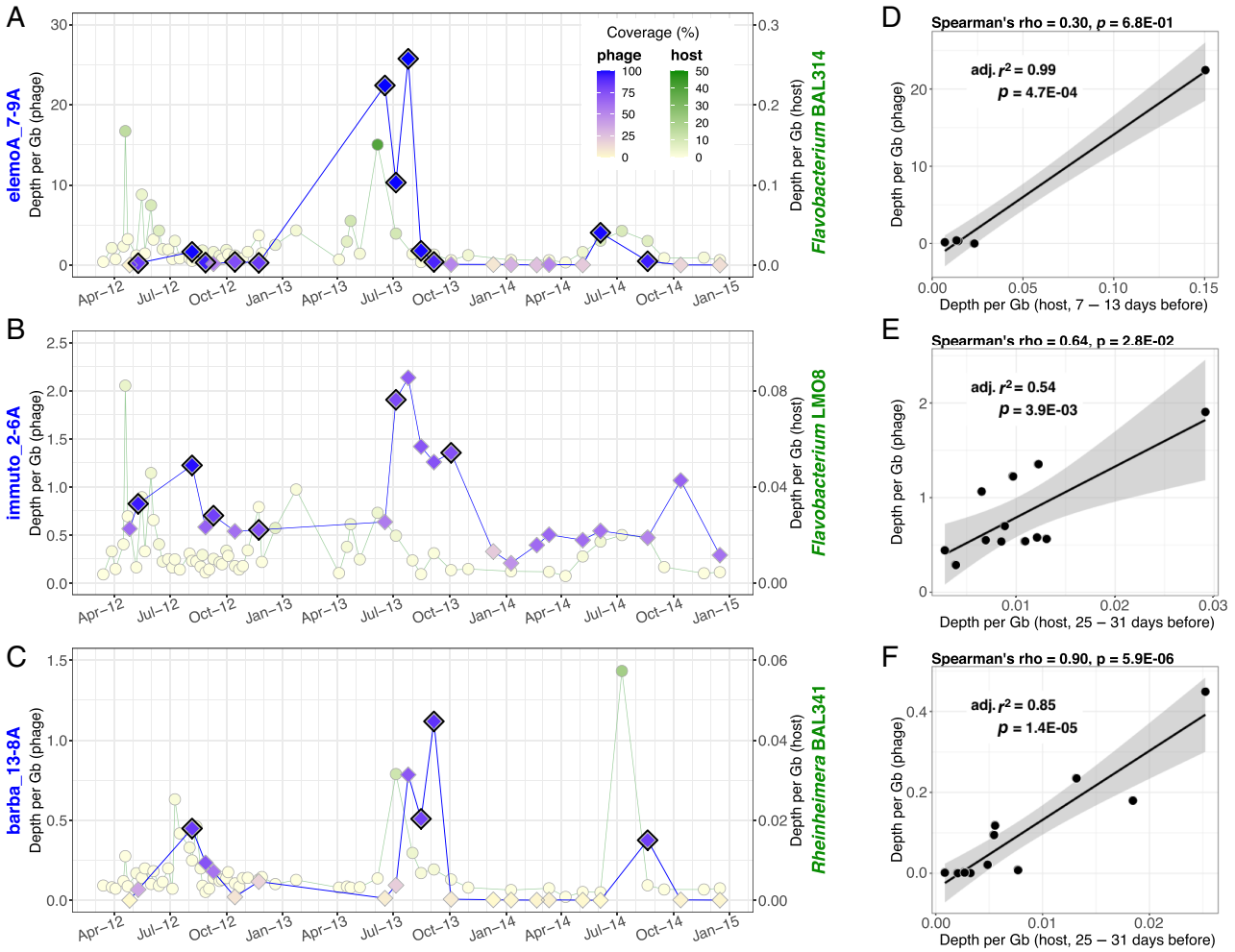

Fig. 8. Detection of phages and their hosts in LMO metagenomes.
(A, B, C) Relative abundance is given as a genome-wide average depth of mapped reads per Gb of metagenome on the *y*-axis (phage—left, host—right). The percentage of the genome covered by at least one mapped read is represented by the colour of each data point. The colour scale, which is given in (A), is the same for all three graphs. Data points of samples with >75% genome coverage are highlighted by black frames. The underlying data are given in Tables S9 and S10.
(D, E, F) Relative abundances of phages versus hosts at the time lag that resulted in the highest adjusted r^2 in linear correlations (see Fig. S2). Associated Spearman rank correlation coefficients are given above each graph. Note that these correlations only provide the first hint on possible time lags between host and phage. Better host detection and shorter sampling intervals are necessary for reliable estimates. [Color figure can be viewed at wileyonlinelibrary.com]

represent an important part of the phage community at LMO during the summer months in terms of abundance.

Despite clear detection of the phages, neither of the three hosts showed >75% coverage in the available metagenomes (0.2–3 μm size fraction) from March 2012 to December 2014 (Fig. 8A–C). The highest genome coverage of BAL314 was only 39%, and the respective depth per Gb was 0.15. Reducing the sequence identity threshold of the mapping from 95% to 80%, which may roughly correspond to genus-level detection, only increased the maximum coverage to 54%, and the corresponding depth per Gb to 0.34 (Table S10), thus, did not result in clear detection either. LMO8 and BAL341 showed even lower detection with the highest genome coverage of only 6% and 21% respectively (Table S10). Despite the weak detection of the hosts, associations between the relative abundance of phage and host were apparent for all three phage–host pairs (Fig. 8, Fig. S2). To get insights into the time-lag of this predator–prey relationship, we correlated host abundances at given time points with phage abundances at later time points (Fig. S2). According to linear regression analysis, a time lag of 7–13 days gave the best correlation between the elemo-phage and BAL314, while a time lag of 25–31 days was suggested between immuto- and barba-phages and their respective hosts (Fig. 8D–F). It should be noted, though, that the mentioned elemo-BAL314 regression (Fig. 8D) is based on only five phage-host abundance pairs, and none of the correlations for this

pair was supported by rank correlations (Fig. S2). The obtained time lag for immuto-LMO8 (Fig. 8E) and barba-BAL341 (Fig. 8F) is better supported, yet, shorter sampling intervals and better detection of the host would be necessary to assess time lags more accurately. However, the results raise the suggestion that the phages might peak up to a month after their host in nature, which contrasts faster succession in mesocosms, where, e.g. barba-phages that responded to agricultural river input were clearly detected 1 week after nutrient addition (Fig. 2C).

The weak detection of the hosts is puzzling, given the clear detection of the phages in the viral metagenomes and especially the high relative abundances of elemo-phages. It cannot be excluded that the principal hosts of these phages in nature are distantly related to BAL314 and corresponding reads were thus hardly recruited even by mapping with an 80% similarity threshold, although plaque assays did not suggest a broad host range. Alternatively, host cells might be predominantly particle associated and thus partly removed in the 3.0 μm prefiltered metagenomes. In an amplicon dataset (V3–V4 region of the 16S rRNA gene) from LMO, the ASV with sequence identity to BAL314 and LMO8 showed on average higher relative abundance in the >3.0 μm compared to the 0.2–3.0 μm size fraction (Table S11). Particle association and responsiveness to phytoplankton blooms have been seen previously for various *Flavobacteriaceae* (Pinhassi *et al*., 2004; Fandino *et al*., 2005; Fernández-Gómez *et al*., 2013), and members of this family are recognized degraders of high molecular weight compounds, such as polysaccharides and peptides (Teeling *et al*., 2012, 2016). Phytoplankton blooms in spring and summer that recurred yearly from 2011 to 2014 at LMO (Bunse *et al*., 2019) might have promoted *Flavobacterium* host strain abundances and thus the recurring viral abundance peaks. The elemo-phages showed noticeable abundance between June and August in three consecutive years (Fig. 8A; Table S9), and pronounced peaks in summer 2013 concurring with distinct cyanobacterial blooms (Bunse *et al*., 2019). The induced phytoplankton blooms, or respectively the addition of cyanobacterial lysate, seemed to promote elemo-phage abundance also in the mesocosms (Fig. 2). Thus, these phages may impact microbial succession during and after phytoplankton blooms, e.g. by shunting compounds degraded by their host to the dissolved organic matter pool (Wilhelm and Suttle, 1999) and thereby enabling the rise of other heterotrophic prokaryotes.

Conclusion

In this study, we genomically characterized isolated phages from the Baltic Proper and traced abundances in a mesocosm experiment and their natural environment. *Rheinheimera* phages of the genus *Barbavirus* were previously shown to seasonally peak in abundance in the Baltic Sea. These 'phage blooms' could be induced in the mesocosm experiment by the addition of nutrient-rich agricultural influenced river water. Near genome identity of mesocosm isolates to previously isolated barba-phages uncovered genomic consistency within this population. In contrast to the almost identical phages obtained in different years, we isolated phages on the *Flavobacterium* strain LMO8 that represents a novel genus (Immutovirus) without similarity to phages previously isolated on this particular host. The genomic features of the immuto-phage provide novel insights on how phages might modulate their hosts during infection through cell surface modification and disclosed an additional phage genus that possesses a gene set coding for synthesis of hypermodified nucleotides. Phages isolated on *Flavobacterium* strain BAL314 represent another novel genus (Elemovirus). The nutrient amended mesocosms revealed pronounced abundance dynamics of these phages, while observed microdiversity was largely maintained during the mesocosm experiment and across different treatments. In their natural environment, the observed seasonal reoccurrence of the elemo-phages suggests a potential influence on microbial succession in response to phytoplankton blooms. While fast responses of increased phage abundances were noted in the mesocosms (within 9 days), metagenomic data from the Baltic Sea hint at a time lag of up to 1 month between host and phage dynamics. In summary, this study provides an integral approach towards a better understanding of how phages impact and are impacted by the recurrent seasonal succession patterns in the Baltic Sea. However, the bulk of phage–host interrelations in this ecosystem remains uncharted and warrants further research.

Acknowledgements

We would like to thank Sabina Arnautovic for isolation of bacterial strains and Zainab Zafar for helping with phage host range tests. We further acknowledge the National Genomics Infrastructure funded by Science for Life Laboratory, the Knut and Alice Wallenberg Foundation and the Swedish Research Council, and SNIC/Uppsala Multidisciplinary Center for Advanced Computational Science for assistance with massively parallel sequencing and access to the UPPMAX computational infrastructure. The data handling was enabled by resources provided by the Swedish National Infrastructure for Computing (SNIC) at UPPMAX partially funded by the Swedish Research Council through grant agreement no. 2018-05973. The project was funded by a grant from the Swedish Research Council (2013-4554) to K.H. and a grant from the Crafoord Foundation (CR2019-0034) to M.H. The research was supported by the BONUS BLUEPRINT project, which has received funding from BONUS, the joint Baltic Sea research and development

programme (Art 185) and the Swedish research council FORMAS. This study was also funded by the strategic research environment EcoChange.

References

Abuladze, N.K., Gingery, M., Tsai, J., and Eiserling, F.A. (1994) Tail length determination in bacteriophage T4. *Virology* **199**: 301–310.

Agarwala, R., Barrett, T., Beck, J., Benson, D.A., Bollin, C., Bolton, E., *et al*. (2018) Database resources of the National Center for Biotechnology Information. *Nucleic Acids Res* **46**: D8–D13.

Allison, G.E., and Verma, N.K. (2000) Serotype-converting bacteriophages and O-antigen modification in *Shigella flexneri*. *Trends Microbiol* **8**: 17–23.

Alneberg, J., Bennke, C., Beier, S., Bunse, C., Quince, C., Ininbergs, K., *et al*. (2020) Ecosystem-wide metagenomic binning enables prediction of ecological niches from genomes. *Commun Biol* **3**: 1–10.

Alonso-Sáez, L., Morán, X.A.G., and Clokie, M.R. (2018) Low activity of lytic pelagiphages in coastal marine waters. *ISME J* **12**: 2100–2102.

Andrews, S. (2010) FastQC: A quality control tool for high throughput sequence data.

Arndt, D., Grant, J.R., Marcu, A., Sajed, T., Pon, A., Liang, Y., and Wishart, D.S. (2016) PHASTER: a better, faster version of the PHAST phage search tool. *Nucleic Acids Res* **44**: W16–W21.

Avrani, S., Wurtzel, O., Sharon, I., Sorek, R., and Lindell, D. (2011) Genomic island variability facilitates *Prochlorococcus*–virus coexistence. *Nature* **474**: 604–608.

Bankevich, A., Nurk, S., Antipov, D., Gurevich, A.A., Dvorkin, M., Kulikov, A.S., *et al*. (2012) SPAdes: a new genome assembly algorithm and its applications to single-cell sequencing. *J Comput Biol* **19**: 455–477.

Berg, K.A., Lyra, C., Sivonen, K., Paulin, L., Suomalainen, S., Tuomi, P., and Rapala, J. (2009) High diversity of cultivable heterotrophic bacteria in association with cyanobacterial water blooms. *ISME J* **3**: 314–325.

Berman, H.M., Westbrook, J., Feng, Z., Gilliland, G., Bhat, T. N., Weissig, H., *et al*. (2000) The protein data bank. *Nucleic Acids Res* **28**: 235–242.

Bischoff, V., Bunk, B., Meier-Kolthoff, J.P., Spröer, C., Poehlein, A., Dogs, M., *et al*. (2019) Cobaviruses – a new globally distributed phage group infecting Rhodobacteraceae in marine ecosystems. *ISME J* **13**: 1404–1421.

Bolger, A.M., Lohse, M., and Usadel, B. (2014) Trimmomatic: a flexible trimmer for Illumina sequence data. *Bioinformatics* **30**: 2114–2120.

Bolyen, E., Rideout, J.R., Dillon, M.R., Bokulich, N.A., Abnet, C.C., Al-Ghalith, G.A., *et al*. (2019) Reproducible, interactive, scalable and extensible microbiome data science using QIIME 2. *Nat Biotechnol* **37**: 852–857.

Brum, J.R., Ignacio-Espinoza, J.C., Roux, S., Doulcier, G., Acinas, S.G., Alberti, A., *et al*. (2015) Patterns and ecological drivers of ocean viral communities. *Science* **348**: 1261498.

Buchfink, B., Xie, C., and Huson, D.H. (2015) Fast and sensitive protein alignment using DIAMOND. *Nat Methods* **12**: 59–60.

Bunse, C., Israelsson, S., Baltar, F., Bertos-Fortis, M., Fridolfsson, E., Legrand, C., *et al*. (2019) High frequency multi-year variability in Baltic Sea microbial plankton stocks and activities. *Front Microbiol* **9**: 3296.

Camacho, C., Coulouris, G., Avagyan, V., Ma, N., Papadopoulos, J., Bealer, K., and Madden, T.L. (2009) BLAST+: architecture and applications. *BMC Bioinformatics* **10**: 421.

Coutinho, F.H., Silveira, C.B., Gregoracci, G.B., Thompson, C.C., Edwards, R.A., Brussaard, C.P.D., *et al*. (2017) Marine viruses discovered via metagenomics shed light on viral strategies throughout the oceans. *Nat Commun* **8**: 15955.

Fandino, L., Riemann, L., Steward, G., and Azam, F. (2005) Population dynamics of Cytophaga-Flavobacteria during marine phytoplankton blooms analyzed by real-time quantitative PCR. *Aquat Microb Ecol* **40**: 251–257.

Fernández-Gómez, B., Richter, M., Schüler, M., Pinhassi, J., Acinas, S.G., González, J.M., and Pedrós-Alió, C. (2013) Ecology of marine Bacteroidetes: a comparative genomics approach. *ISME J* **7**: 1026–1037.

Finn, R.D., Mistry, J., Tate, J., Coggill, P., Heger, A., Pollington, J.E., *et al*. (2010) The Pfam protein families database. *Nucleic Acids Res* **38**: D211–D222.

Grazziotin, A.L., Koonin, E.V., and Kristensen, D.M. (2017) Prokaryotic Virus Orthologous Groups (pVOGs): a resource for comparative genomics and protein family annotation. *Nucleic Acids Res* **45**: D491–D498.

Gregory, A.C., Zayed, A.A., Conceição-Neto, N., Temperton, B., Bolduc, B., Alberti, A., *et al*. (2019) Marine DNA viral macro- and microdiversity from pole to pole. *Cell* **177**: 1109–1123.e14.

Harrison, A.O., Moore, R.M., Polson, S.W., and Wommack, K.E. (2019) Reannotation of the ribonucleotide reductase in a cyanophage reveals life history strategies within the virioplankton. *Front Microbiol* **10**: 134.

Highfield, A., Joint, I., Gilbert, J.A., Crawfurd, K.J., and Schroeder, D.C. (2017) Change in *Emiliania huxleyi* virus assemblage diversity but not in host genetic composition during an ocean acidification mesocosm experiment. *Viruses* **9**: 41.

Hofer, A., Crona, M., Logan, D.T., and Sjöberg, B.-M. (2012) DNA building blocks: keeping control of manufacture. *Crit Rev Biochem Mol Biol* **47**: 50–63.

Holmfeldt, K., Middelboe, M., Nybroe, O., and Riemann, L. (2007) Large variabilities in host strain susceptibility and phage host range govern interactions between lytic marine phages and their flavobacterium hosts. *Appl Environ Microbiol* **73**: 6730–6739.

Holmfeldt, K., Solonenko, N., Shah, M., Corrier, K., Riemann, L., VerBerkmoes, N.C., and Sullivan, M.B. (2013) Twelve previously unknown phage genera are ubiquitous in global oceans. *Proc Natl Acad Sci U S A* **110**: 12798–12803.

Hugerth, L.W., Larsson, J., Alneberg, J., Lindh, M.V., Legrand, C., Pinhassi, J., and Andersson, A.F. (2015) Metagenome-assembled genomes uncover a global brackish microbiome. *Genome Biol* **16**: 279.

Hurwitz, B.L., and Sullivan, M.B. (2013) The Pacific Ocean Virome (POV): a marine viral metagenomic dataset and associated protein clusters for quantitative viral ecology. *PLoS One* **8**: e57355.

Hutinet, G., Kot, W., Cui, L., Hillebrand, R., Balamkundu, S., Gnanakalai, S., *et al*. (2019) 7-Deazaguanine modifications protect phage DNA from host restriction systems. *Nat Commun* **10**: 1–12.

Iseki, S., and Sakai, T. (1953) Artificial transformation of O antigens in Salmonella E group. II. Antigen-transforming factor in *Bacilli* of subgroup E_2. *Proc Jpn Acad* **29**: 127–131.

Kang, I., Oh, H.-M., Kang, D., and Cho, J.-C. (2013) Genome of a SAR116 bacteriophage shows the prevalence of this phage type in the oceans. *Proc Natl Acad Sci U S A* **110**: 12343–12348.

Karlsson, C.M.G., Cerro-Gálvez, E., Lundin, D., Karlsson, C., Vila-Costa, M., and Pinhassi, J. (2019) Direct effects of organic pollutants on the growth and gene expression of the Baltic Sea model bacterium Rheinheimera sp. BAL341. *J Microbial Biotechnol* **12**: 892–906.

Katoh, K., and Standley, D.M. (2013) MAFFT multiple sequence alignment software version 7: improvements in performance and usability. *Mol Biol Evol* **30**: 772–780.

Katsura, I., and Hendrix, R.W. (1984) Length determination in bacteriophage lambda tails. *Cell* **39**: 691–698.

Kauffman, K.M., and Polz, M.F. (2018) Streamlining standard bacteriophage methods for higher throughput. *MethodsX* **5**: 159–172.

Kropinski, A.M., Prangishvili, D., and Lavigne, R. (2009) Position paper: the creation of a rational scheme for the nomenclature of viruses of Bacteria and Archaea. *Environ Microbiol* **11**: 2775–2777.

Langmead, B., and Salzberg, S.L. (2012) Fast gapped-read alignment with Bowtie 2. *Nat Methods* **9**: 357–359.

Lefort, V., Desper, R., and Gascuel, O. (2015) FastME 2.0: a comprehensive, accurate, and fast distance-based phylogeny inference program. *Mol Biol Evol* **32**: 2798–2800.

Li, X., Gerlach, D., Du, X., Larsen, J., Stegger, M., Kühner, P., *et al*. (2015) An accessory wall teichoic acid glycosyltransferase protects *Staphylococcus aureus* from the lytic activity of Podoviridae. *Sci Rep* **5**: 17219.

Lindh, M.V., Figueroa, D., Sjöstedt, J., Baltar, F., Lundin, D., Andersson, A., *et al*. (2015) Transplant experiments uncover Baltic Sea basin-specific responses in bacterioplankton community composition and metabolic activities. *Front Microbiol* **6**: 223.

López-Pérez, M., Martin-Cuadrado, A.-B., and Rodriguez-Valera, F. (2014) Homologous recombination is involved in the diversity of replacement flexible genomic islands in aquatic prokaryotes. *Front Genet* **5**: 147.

Lowe, T.M., and Chan, P.P. (2016) tRNAscan-SE On-line: integrating search and context for analysis of transfer RNA genes. *Nucleic Acids Res* **44**: W54–W57.

Lundin, D., Torrents, E., Poole, A.M., and Sjöberg, B.-M. (2009) RNRdb, a curated database of the universal enzyme family ribonucleotide reductase, reveals a high level of misannotation in sequences deposited to Genbank. *BMC Genomics* **10**: 589.

Mahony, J., Alqarni, M., Stockdale, S., Spinelli, S., Feyereisen, M., Cambillau, C., and van Sinderen, D. (2016) Functional and structural dissection of the tape measure protein of lactococcal phage TP901-1. *Sci Rep* **6**: 1–10.

Markine-Goriaynoff, N., Gillet, L., Van Etten, J.L., Korres, H., Verma, N., and Vanderplasschen, A. (2004) Glycosyltransferases encoded by viruses. *J Gen Virol* **85**: 2741–2754.

Markowitz, V.M., Chen, I.-M.A., Palaniappan, K., Chu, K., Szeto, E., Grechkin, Y., *et al*. (2012) IMG: the integrated microbial genomes database and comparative analysis system. *Nucleic Acids Res* **40**: D115–D122.

Marston, M.F., and Martiny, J.B.H. (2016) Genomic diversification of marine cyanophages into stable ecotypes. *Environ Microbiol* **18**: 4240–4253.

Martin, M. (2011) Cutadapt removes adapter sequences from high-throughput sequencing reads. *EMBnetjournal* **17**: 10–12.

Martínez-Carranza, M., Jonna, V.R., Lundin, D., Sahlin, M., Carlson, L.-A., Jemal, N., *et al*. (2020) A ribonucleotide reductase from Clostridium botulinum reveals distinct evolutionary pathways to regulation via the overall activity site. *J Biol Chem* **295**: 15576–15587.

Martinez-Hernandez, F., Fornas, O., Gomez, M.L., Bolduc, B., de la Cruz Peña, M.J., Martínez, J.M., *et al*. (2017) Single-virus genomics reveals hidden cosmopolitan and abundant viruses. *Nat Commun* **8**: 1–13.

McNair, K., Zhou, C., Dinsdale, E.A., Souza, B., and Edwards, R.A. (2019) PHANOTATE: a novel approach to gene identification in phage genomes. *Bioinformatics* **35**: 4537–4542.

Meier-Kolthoff, J.P., and Göker, M. (2017) VICTOR: genome-based phylogeny and classification of prokaryotic viruses. *Bioinformatics* **33**: 3396–3404.

Moraru, C., Varsani, A., and Kropinski, A.M. (2020) VIRIDIC - a novel tool to calculate the intergenomic similarities of prokaryote-infecting viruses. *Viruses* **12**: 1268.

Nilsson, E., Bayfield, O.W., Lundin, D., Antson, A.A., and Holmfeldt, K. (2020) Diversity and host interactions among virulent and temperate baltic sea flavobacterium phages. *Viruses* **12**: 158.

Nilsson, E., Li, K., Fridlund, J., Šulčius, S., Bunse, C., Karlsson, C.M.G., *et al*. (2019) Genomic and seasonal variations among aquatic phages infecting the Baltic Sea Gammaproteobacterium *Rheinheimera* sp. strain BAL341. *Appl Environ Microbiol* **85**: e01003-19.

Osbeck, C. (2019) *Exploring gene expression responses of marine bacteria to environmental factors*: Växjö: Linnaeus University Press.

Øvreås, L., Bourne, D., Sandaa, R.-A., Casamayor, E.O., Benlloch, S., Goddard, V., *et al*. (2003) Response of bacterial and viral communities to nutrient manipulations in seawater mesocosms. *Aquat Microb Ecol* **31**: 109–121.

Page, A.J., Cummins, C.A., Hunt, M., Wong, V.K., Reuter, S., Holden, M.T.G., *et al*. (2015) Roary: rapid large-scale prokaryote pan genome analysis. *Bioinformatics* **31**: 3691–3693.

Pedulla, M.L., Ford, M.E., Houtz, J.M., Karthikeyan, T., Wadsworth, C., Lewis, J.A., *et al*. (2003) Origins of highly mosaic mycobacteriophage genomes. *Cell* **113**: 171–182.

Pinhassi, J., Sala, M.M., Havskum, H., Peters, F., Guadayol, Ò., Malits, A., and Marrasé, C. (2004) Changes

in Bacterioplankton composition under different phytoplankton regimens. *Appl Environ Microbiol* **70**: 6753–6766.

Pritchard, L., Glover, R.H., Humphris, S., Elphinstone, J.G., and Toth, I.K. (2015) Genomics and taxonomy in diagnostics for food security: soft-rotting enterobacterial plant pathogens. *Anal Methods* **8**: 12–24.

R Core Team. (2019) *R: a language and environment for statistical computing*. Vienna, Austria: R Foundation for Statistical Computing.

Richter, M., and Rosselló-Móra, R. (2009) Shifting the genomic gold standard for the prokaryotic species definition. *Proc Natl Acad Sci U S A* **106**: 19126–19131.

Rodriguez-Valera, F., Martin-Cuadrado, A.-B., and López-Pérez, M. (2016) Flexible genomic islands as drivers of genome evolution. *Curr Opin Microbiol* **31**: 154–160.

Rodriguez-Valera, F., Martin-Cuadrado, A.-B., Rodriguez-Brito, B., Pašić, L., Thingstad, T.F., Rohwer, F., and Mira, A. (2009) Explaining microbial population genomics through phage predation. *Nat Rev Microbiol* **7**: 828–836.

Roux, S., Emerson, J.B., Eloe-Fadrosh, E.A., and Sullivan, M.B. (2017). Benchmarking viromics: an in silico evaluation of metagenome-enabled estimates of viral community composition and diversity. *PeerJ* **5**: e3817.

Sandaa, R.-A., Gómez-Consarnau, L., Pinhassi, J., Riemann, L., Malits, A., Weinbauer, M.G., *et al*. (2009) Viral control of bacterial biodiversity – evidence from a nutrient-enriched marine mesocosm experiment. *Environ Microbiol* **11**: 2585–2597.

Schroeder, D.C., Oke, J., Hall, M., Malin, G., and Wilson, W. H. (2003) Virus succession observed during an Emiliania huxleyi Bloom. *Appl Environ Microbiol* **69**: 2484–2490.

Stamatakis, A. (2014) RAxML version 8: a tool for phylogenetic analysis and post-analysis of large phylogenies. *Bioinformatics* **30**: 1312–1313.

Straub, D., Blackwell, N., Langarica-Fuentes, A., Peltzer, A., Nahnsen, S., and Kleindienst, S. (2020) Interpretations of environmental microbial community studies are biased by the selected 16S rRNA (Gene) amplicon sequencing pipeline. *Front Microbiol* **11**: 550420.

Šulčius, S., and Holmfeldt, K. (2016) Viruses of microorganisms in the Baltic Sea: current state of research and perspectives. *Mar Biol Res* **12**: 115–124.

Suttle, C.A. (1994) The significance of viruses to mortality in aquatic microbial communities. *Microb Ecol* **28**: 237–243.

Tatusov, R.L., Galperin, M.Y., Natale, D.A., and Koonin, E.V. (2000) The COG database: a tool for genome-scale analysis of protein functions and evolution. *Nucleic Acids Res* **28**: 33–36.

Teeling, H., Fuchs, B.M., Becher, D., Klockow, C., Gardebrecht, A., Bennke, C.M., *et al*. (2012) Substrate-controlled succession of marine bacterioplankton populations induced by a phytoplankton bloom. *Science* **336**: 608–611.

Teeling, H., Fuchs, B.M., Bennke, C.M., Krüger, K., Chafee, M., Kappelmann, L., *et al*. (2016) Recurring patterns in bacterioplankton dynamics during coastal spring algae blooms. *Elife* **5**: e11888.

Turner, B., Burkhart, B.W., Weidenbach, K., Ross, R., Limbach, P.A., Schmitz, R.A., *et al*. (2020) Archaeosine modification of archaeal tRNA: role in structural stabilization. *J Bacteriol* **202**: e00748-19.

Wang, X., Matuszek, Z., Huang, Y., Parisien, M., Dai, Q., Clark, W., *et al*. (2018) Queuosine modification protects cognate tRNAs against ribonuclease cleavage. *RNA* **24**: 1305–1313.

Wilhelm, S.W., and Suttle, C.A. (1999) Viruses and nutrient cycles in the seaviruses play critical roles in the structure and function of aquatic food webs. *Bioscience* **49**: 781–788.

Zhao, Y., Temperton, B., Thrash, J.C., Schwalbach, M.S., Vergin, K.L., Landry, Z.C., *et al*. (2013) Abundant SAR11 viruses in the ocean. *Nature* **494**: 357–360.

Zimmermann, L., Stephens, A., Nam, S.-Z., Rau, D., Kübler, J., Lozajic, M., *et al*. (2018) A completely reimplemented MPI bioinformatics toolkit with a new HHpred server at its core. *J Mol Biol* **430**: 2237–2243.

Supporting Information

Additional Supporting Information may be found in the online version of this article at the publisher's web-site:

Supporting Information S1. Supporting Information for Environmental Microbiology.

Table S1. Plaque-forming units (PFU) per ml obtained during the mesocosm experiment. 400 μl of mesocosm water were used for each sample, thus, PFU ml^{-1} values can be fractional numbers.

Table S2. Inter-genomic similarities among immuto- and elemo-phages calculated using VIRIDIC.

Table S3. Inter-genomic similarities among barba-phages calculated using VIRIDIC.

Table S4. Genome annotation of vB_FspM_immuto_2-6A.

Table S5. Genome annotation of vB_FspP_elemoA_7-9A.

Table S6. Accessory genome of the elemo-phages isolated in this study.

Table S7. Genome annotation of vB_FspM_barba13-8A.

Table S8 Tape measure protein (TMP) and tail lengths of various Sipho- and Myoviridae phages.

Table S9. Results from Bowtie2 mapping of LMO viral metagenomes (<0.2 μm size fraction) against the genomes of the phages elemoA_7-9A, immuto_2-6A, and barba_13-8A.

Table S10. Results from Bowtie2 mapping of LMO metagenomes (0.2–3 μm size fraction) against the genomes of Flavobacterium strains BAL314 and LMO8 and Rheinheimera strain BAL341.

Table S11. Detection of the amplicon sequence variant (ASV) that comprises both Flavobacterium strains BAL314 and LMO8 in different filter size fractions of samples from LMO surface water (2012–2015). The average relative abundance of the ASV was higher in the >3 μm size fraction than in the 3 μm prefiltered samples.